REVIEW

ACS chemical biology

A Survey of Single-Molecule Techniques in Chemical Biology

Peter V. Cornish[†] and Taekjip Ha[‡,*]

[†]Department of Physics, [‡]Howard Hughes Medical Institute, University of Illinois, Urbana–Champaign, 1110 West Green Street, Urbana, Illinois 61801-3080

ABSTRACT Single-molecule methods have revolutionized scientific research by rendering the investigation of once-inaccessible biological processes amenable to scientific inquiry. Several of the more established techniques will be emphasized in this Review, including single-molecule fluorescence microscopy, optical tweezers, and atomic force microscopy, which have been applied to many diverse biological processes. Serving as a taste of all the exciting research currently underway, recent examples will be discussed of translocation of RNA polymerase, myosin VI walking, protein folding, and enzyme activity. We will end by providing an assessment of what the future holds, including techniques that are currently in development.

The popularity of single-molecule experiments has grown tremendously over the last two decades. The number of papers published per year since 1987 with "single molecule" in the title, according to a search on PubMed (www.pubmed.gov), is shown (Figure 1). The number of publications for 2006, 315, is a projection based on the first 7 months of the year. These numbers are gross underestimates (*e.g.*, only 9 of the 43 references in this Review would turn up in such a search), but the growth pattern may still be grasped. The search found virtually no papers in the 1980s despite the fact that the first single-molecule measurements were done on single-ion channels and were already widespread by that time. The growth shown (Figure 1) appears exponential, with a doubling time of 2.2 years. We can predict that in 30 years, every paper published in the biological sciences will be on single-molecule techniques! In more serious terms, single-molecule approaches to biology have become enormously popular because of their power in providing previously unattainable data on elementary biological processes. The two primary approaches are fluorescence and manipulation (force). Fluorescence includes FRET, polarization, lifetime, localization, and intensity, whereas manipulation includes optical and magnetic tweezers and atomic force microscopy (AFM). Here, we will discuss only localization and intensity for fluorescence and optical tweezers and AFM for manipulation, and we refer readers to review papers for other techniques not discussed here (*1*–*9*).

The two common experimental setups for measuring fluorescence at the single-molecule level are confocal microscopy (Figure 2, panel a) and total internal reflection fluorescence (TIRF) microscopy (Figure 2, panel b). In confocal microscopy, a laser is focused through the objective lens of a microscope, exciting only a small

*Corresponding author, tjha@uiuc.edu.

Received for review August 6, 2006 and accepted September 25, 2006.

Published online January 19, 2007

10.1021/cb600342a CCC: $37.00

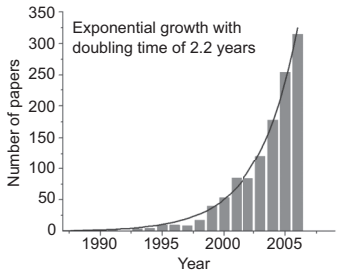

Figure 1. The occurrence in the scientific literature of papers on single-molecule methods. The number is calculated from a PubMed search displayed as a function of the year from the 1980s until the end of 2006.

volume. The emission can be split into multiple channels for acquisition. To image many molecules, a piezo stage is typically used to scan the slide. The benefit of confocal microscopy is that a time resolution on the order of microseconds can be achieved. The two types of TIRF commonly used differ only by how the excitation light is brought to the sample: either through a prism (Figure 2, panel b) or directly through the objective. An evanescent wave is created that excites only those molecules within a few hundred nanometers of the quartz surface. The fluorescence emission is then sent through the objective and is recorded on a CCD camera. The benefit of TIRF over confocal microscopy is that a larger area of the slide can be imaged simultaneously, and this provides more data quickly. The drawback of this method is that the camera limits the time resolution, which in some cases is as short as a few milliseconds.

The resolution and application of optical tweezers experiments have improved significantly over the last several years (*10*–*12*). Experiments performed with optical tweezers are designed to have two attachment points with several variations (Figure 3, panels a and b).

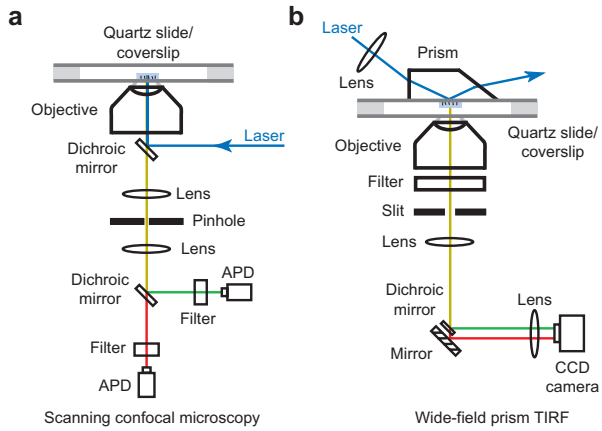

Figure 2. Conventional experimental setups used for single-molecule fluorescence. a) A typical confocal microscope with both the excitation light and emission going through the objective lens. APD = avalanche photodiode. b) A prism-type TIRF microscope where the excitation light is reflected through a prism on top of the slide and the emission goes through the objective.

Usually, biotin–avidin chemistry is used to link one of the attachment points to a polystyrene bead. This bead is trapped in a laser beam. The other attachment point can be either linked to another bead that is trapped in a second laser beam (Figure 3, panel a), attached to the slide surface, or captured by a micropipet (Figure 3, panel b). These setups can be used to measure force extension curves as molecules are pulled apart or to watch a change in distance as the beads are pulled together by the attached molecules. Using optical tweezers offers several benefits, including the method's adaptability and its high accuracy in distance changes. The dual-beam trap is much less prone to mechanical drift and beam-pointing instability than the single-beam trap, but the linkage between the two beads should be long enough to trap them independently. Because the resolution will ultimately be determined by the compliance of the linker molecules, the single-beam trap, which can use arbitrarily short linkers, may indeed achieve better resolution, as long as the mechanical drift is avoided by extremely careful design of the apparatus.

AFM is a scanning probe microscopy technique that has been around for 2 decades. Although AFM has typically been used for topographical imaging applications, it has found uses in manipulating samples of all kinds, including in biological studies to look at the folding and unfolding of molecules. A typical AFM is a simple apparatus that consists of a cantilever with an attached tip, which is used to directly interact with the sample (Figure 3, panel c). For detection, a laser is deflected off the cantilever, and a positional detector is used to record the change in vertical distance. In this way, force extension curves can be created to measure the change in force over distance. A sensitivity of 1 pN and spatial resolution of 1 nm can be achieved with this technique (*4*). The benefit of AFM over optical tweezers is that AFM is capable of much higher forces, allowing for the study of larger molecules or polymers. The drawback to AFM is that the force noise is higher than that in optical tweezers and can still be a few piconewtons in the best instrumental setups (*13*).

Overview of Recent Reports on Single-Molecule Methods. Single-molecule methods have been applied to biology and chemistry in numerous ways; it would be impossible to review here all of the studies performed in the last few years. Several recent studies have been chosen that illustrate the diversity of single-molecule methods and show that many different biological pro-

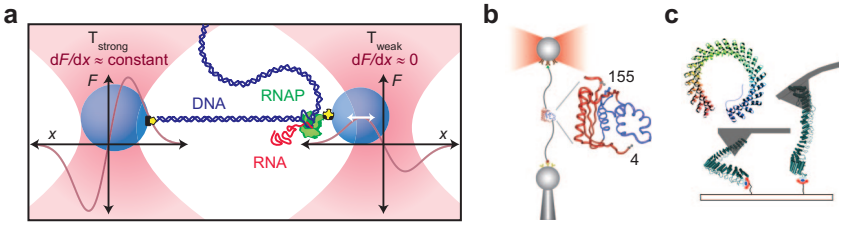

Figure 3. Mechanical force single-molecule techniques. a) Dumb-bell-type optical tweezers suspending a stalled RNA polymerase transcription complex. Adapted by permission from Macmillan Publishers Ltd., copyright 2005 (*11*). b) Optical tweezers experimental design with one bead trapped in a laser and the other immobilized with a micropipet pulling on a single RNase H molecule. Reprinted by permission from AAAS, copyright 2005 (*26*). c) AFM experiment pulling on a poly-ankyrin molecule. The cantilever and attached tip are shown in gray. Reprinted by permission from Macmillan Publishers Ltd., copyright 2006 (*31*).

cesses can be approached by these powerful techniques. Some recent papers relating to motor proteins demonstrate the precision and spatial resolution that can be attained from these methods. Folding and unfolding studies of proteins describe the potential of mechanical force for elucidating the folding landscape of molecules. The study of enzymatic turnover of substrates by single enzymes allows scientists not only to delve into individual reactions but also to investigate the possibility of memory effects in proteins.

RNA Polymerase Translocation and Pausing. RNA polymerase is a ubiquitous enzyme found in all forms of life. In *Escherichia coli*, RNA polymerase exists as a multisubunit protein with a core of four subunits ($\alpha_2\beta\beta'$), and it also contains one of seven σ factor subunits that recognize specific promoter regions (*14*). It functions by unraveling double-stranded DNA (dsDNA), allowing the sense strand to be transcribed into RNA by adding the cognate ribonucleoside monophosphate as it progresses. The detailed process of translocation of RNA polymerase at the molecular level has been debated for many years, and several models have been proposed to explain this highly regulated process (*11, 15*). Several recent single-molecule studies have shown intricate and detailed aspects of initiation, translocation, and pausing of RNA polymerase from *E. coli* (*11, 16, 17*).

In order to investigate the small discrete steps taken by RNA polymerase during each elongation cycle, scientists constructed a very sensitive and ultrastable optical trap that was capable of angstrom-level resolution. A dumbbell setup was used in which two polystyrene beads were trapped in separate laser beams (Figure 3, panel a) (*18*). With this technique, the molecule of interest is suspended over the slide surface to eliminate any fluctuations from stage drift. To reduce fluctuations from laser pointing, all of the components were enclosed in a box purged with helium. Researchers realized a 10-fold reduction of noise spectral density at 0.1 Hz solely by switching from air to helium (*11*).

In the first of these studies (*11*), the β′-subunit of a stalled RNA polymerase transcription complex is attached directly to a polystyrene bead through an avidin linkage (Figure 3, panel a). Depending on the experiment, either the upstream or downstream portion of the DNA is then attached to another polystyrene bead with a digoxigenin antibody linkage. Under experimentally determined concentrations of ribonucleoside triphosphates that produce an optimal level of RNA polymerase movement, individual steps of translocation were observed. The step size for each round of translocation was calculated to be 3.7 ± 0.6 Å (Figure 4, panel a). This is the distance per base pair of duplex DNA within error.

What types of new scientific questions can be addressed with this ultimate resolution of single base pair in transcription? The same study reported an elegant example. The researchers investigated whether the translocation mechanism of RNA polymerase is driven by a power stroke generated by inorganic pyrophosphate (PP_i) release or whether it occurs through a Brownian ratchet mechanism

KEYWORDS

Atomic force microscopy (AFM): An AFM instrument contains a cantilever that can be used to scan a surface to produce an image, or it can be attached to a molecule and used in pulling experiments. Motions are detected by observing movements of a laser that is deflected off the cantilever.

Fluorescence imaging with one-nanometer accuracy (FIONA): A single-molecule fluorescence technique used to localize individual fluorophores to within ~1.5 nm. This resolution is obtained by analyzing the fluorescence image or point spread function and fitting it to a Gaussian function.

Fluorescence resonance energy transfer (FRET): When a fluorescent dye (donor) is excited by a light source, energy can be transferred nonradiatively to another dye (acceptor), which is within ~2–8 nm. Typically, FRET measurements are performed between two different fluorescent dyes where the emission of the donor dye overlaps the absorption of the acceptor. As the two molecules come closer together, the donor emission decreases in intensity while the acceptor emission increases.

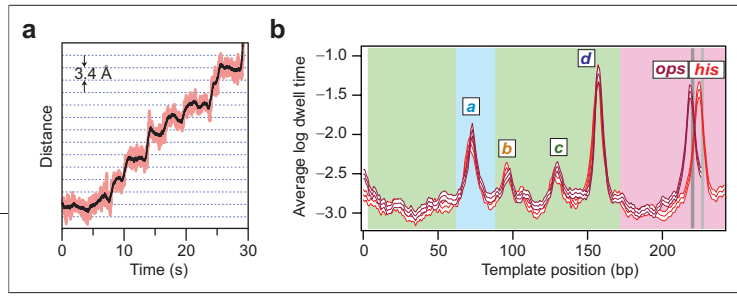

Figure 4. RNA polymerase in motion. a) Individual steps of RNA polymerase during translocation. Adapted by permission from Macmillan Publishers Ltd., copyright 2005 (*11*). b) Detected pausing on two different templates that contain either the *ops* (magenta) or *his* (red) pause site motifs. Four ubiquitous pause sites are also indicated as *a*–*d*. Colors correspond to different regions of the template construct with the *rpoB* gene in green, the restriction sites in light blue, the regulatory pause region in pink, and the *ops* and *his* pause sites in dark gray and light gray, respectively. Reprinted by permission from Elsevier, copyright 2006 (*17*).

by which reversible oscillations between pre- and post-translocation states are trapped by NTP binding. To distinguish between these possible kinetic models of translocation, they recorded the speed of elongation under different forces and NTP concentrations. They concluded that the power stroke model is not valid and that the data favor the Brownian ratchet model in which a secondary NTP binding site could influence translocation at higher NTP concentrations. The ultrahigh resolution was critical in the analysis because frequent pausing and backtracking of RNA polymerase could be filtered out to obtain accurate numbers for the elongation speed.

Single-molecule transcription studies have shown ubiquitous pauses (*19, 20*), but it has not been clear whether these pauses are random events or sequence-dependent. Eight repeats of a DNA motif with two known strong pausing sequences and a termination sequence were incorporated into the DNA to determine the position of the RNA polymerase on the DNA template accurately (*17*). This allows for the rescaling of the experimental data so that the absolute position can be determined. The analysis uncovered four additional ubiquitous pausing sequences and some common features among them, and it became clear that these ubiquitous pause sites are sequence-dependent (Figure 4, panel b).

Because this approach allows a single enzyme to traverse up to eight identical pause sites, the authors could test for molecular memory effects. For example, an enzyme may (i) stay in long-lived states that have different pause tendencies, (ii) switch between states of different pause tendencies during the measurement, or (iii) possess a constant pause propensity. In every corresponding pause site, a positive correlation exists between pausing at one site and pausing at the identical site in a subsequent repeat. This observation and that the correlation between pause sites did not change over at least ~1000 base pairs lend support to the first model. Individual molecules, then, remain in the same state for a long period of time, and it is the molecule itself that determines the kinetics of pausing.

Myosin VI Stepping. Most of the proteins in the myosin family function by moving toward the barbed (+) end of actin filaments. Myosin VI is one exception that moves in the opposite direction or the pointed (−) end. These dimeric processive motor proteins (*21*) are composed of a motor domain, an IQ motif (named for the presence of isoleucine and glutamine) that binds calmodulin, a coiled-coil region, and a globular C-terminal domain. Additionally, myosin VI contains an insertion between the IQ motif and the motor domain, which also binds calmodulin. It was proposed that myosin VI could not function in a lever arm mechanism because its short lever arm would result in a very short step size.

A recently developed single-molecule technique known as fluorescence imaging with one-nanometer accuracy (FIONA) (*22*) was employed to test myosin VI step size (*23, 24*). A standard TIRF setup is used for these experiments (Figure 2, panel b). The basic premise of FIONA is to accurately determine the position of the fluorescent dye in the *x*–*y* plane by curve-fitting the image or point spread function to a Gaussian function. By locating the position of the dye before and after the molecule of interest has moved, the step size can be accurately determined to within ~1.5 nm (*22*). Locating the position of the dye before and after the molecule of interest has moved allows the step size to be accurately determined to within ~1.5 nm (*22*). Two separate constructs were used, one with a Cy3-labeled calmodulin/myosin VI complex and the other with a myosin VI fusion protein with enhanced GFP (eGFP) at the N terminus. The average step size of myosin VI was ~60 nm, an indication that each head of the molecule takes shorter steps of ~30 nm (Figure 5, panel e). This result is consistent with the hand-over-hand mechanism, because an inchworm mechanism would imply that the step size would be only ~30 nm. The authors propose a mechanism of myosin VI movement starting with one bound and one free motor domain (Figure 5, panels a–e). The free motor domain is in the ADP·Pi bound state, and Pi is released upon binding to the actin filament. Once this lead head binds to the actin filament, ADP is released from the rear head. ATP then binds to the rear head and is hydrolyzed, and this allows the rear head to detach from the actin filament. The rear head is then able to swing forward and bind to the actin filament, completing the cycle.

Comparing FIONA with FRET. How is FIONA different from FRET? FIONA measures the location of an object in the laboratory frame with a precision of ~1.5 nm. FRET measures the relative distance of two points in a system in its own center of mass frame with the resolution of ~0.5 nm. Because FRET is sensitive to distances between 2 and 8 nm, it is not suitable for measuring a long-range movement of a motor protein, unlike FIONA, which can measure movements over micrometer or longer length scales. However, FRET is insensitive to the microscope drift because of its ability to measure internal motion, whereas FIONA requires absolute stability. Furthermore, FRET can achieve 0.5-nm resolution with only ~100 photons, whereas FIONA needs 10,000 photons for 1.5-nm precision. For the study of molecular motors, FIONA is suitable only when the track is stiff and straight over a micrometer length scale, whereas FRET can measure movements on a motor with a much more flexible track, such as double- or single-stranded DNA. In the end, these techniques complement each other, although one can probably argue that FRET can be applied more generally to a larger class of biological problems.

RNase H Three-State Folding Mechanism. Ribonuclease (RNase) H from *E. coli* is a relatively small one-domain protein that has been well characterized as a model for protein folding and stability (*25*). The core of the protein is the most stable portion of the molecule, and experiments have shown that it is the first portion to fold and subsequently the last to unfold after the periphery of the protein. Standard experimental methods have so far been unable to fully investigate the presence and contribution of the potential intermediate state in the folding pathway. Single-beam optical tweezers were used to study force-induced unfolding of the molecule in order to probe the intermediate state (*26*). Two ~500 base pair dsDNA handles were attached to distinct positions on opposite sides of RNase H (Figure 3, panel b). Each handle was also independently attached to one of the two polystyrene beads. One of the beads was immobilized by a micropipet, and the other was trapped with a laser.

Two different transitions were observed in the force extension curves when the protein was pulled apart two consecutive times (Figure 6, panel a). The high-force transition (~19 pN) upon the first pull yielded the increase in extension of 50 ± 5 nm; this matched the contour length of the unfolded protein and therefore was interpreted as complete unfolding of RNase H (N → U). After the protein is relaxed to a low force and is stretched again, reversible transitions of ~40 nm in extension were observed at 5.5 pN (I → U); this implied that upon refolding, the protein does not completely return to the native state and that transitions between the folded state and a folding intermediate were occurring. This interpretation was supported by the fact that a longer wait in a low force, or a longer refolding time, restored the high-force transition. Such three-state behavior is also observed at a constant force for which the protein undergoes multiple transitions between the unfolded state and the intermediate state before finally-settling on the native state (Figure 6, panel b); this is analogous to the three-state folding trajectories observed in the single-molecule FRET studies of the hairpin ribozyme (*27*).

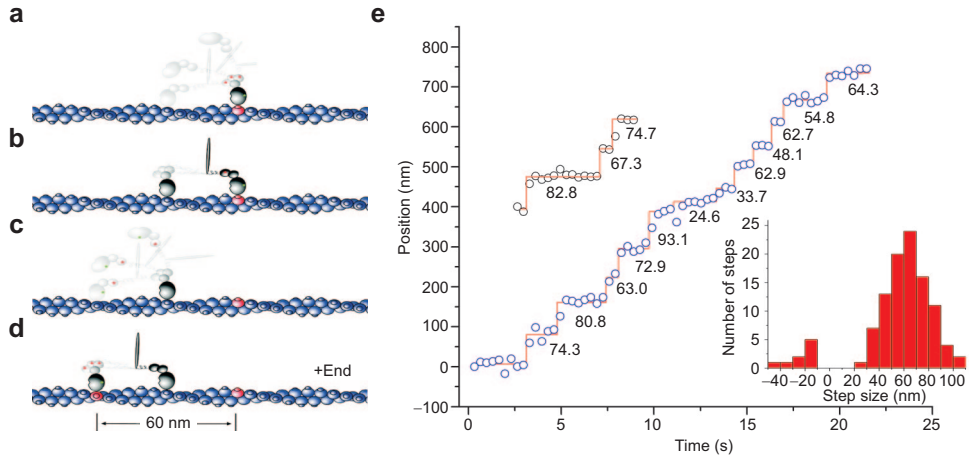

Figure 5. Myosin VI walking. a–d) Proposed mechanism of myosin VI walking hand-over-hand as described in the text. e) Traces showing the individual step size of an eGFP-labeled myosin VI molecule. Histogram of step sizes from multiple molecules, which includes steps in the negative direction (inset). The step size values are in nanometers. Panels a–e reprinted by permission from the American Society for Biochemistry and Molecular Biology, copyright 2004 (*23*).

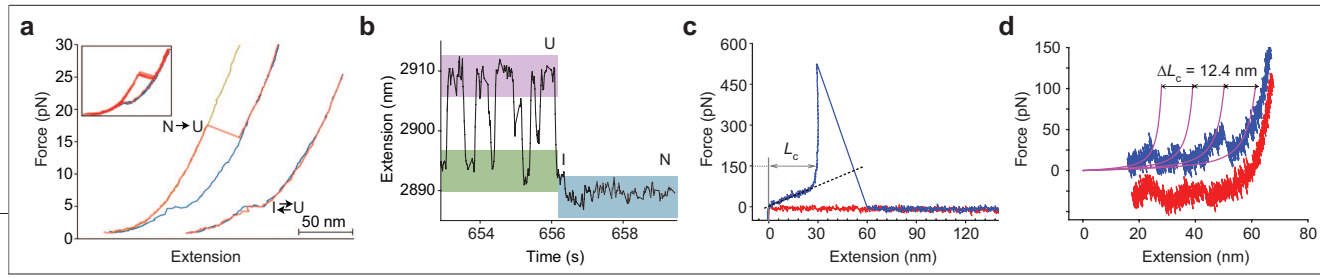

Figure 6. Mechanical force unfolding of RNase H and ankyrin repeats. a) Force extension curves of RNase H showing the high-force (~19 pN) unfolding transition and the lower-force (~5.5 pN) folding/unfolding transition. b) Fluctuations of RNase H at a constant applied force between the unfolded state (red) and the intermediate state (green). After multiple fluctuations, a compaction of the molecule occurs, restoring it to the native state (blue). Panels a and b reprinted by permission from AAAS, copyright 2005 (*26*). c) Representative unfolding of an ankyrin polymer, with unfolding in blue and refolding in red. The linear phase is indicative of the spring properties of the molecule. d) After unfolding of the polymer as in panel c, some molecules exhibited unfolding transitions indicative of individual repeats. Panels c and d reprinted by permission from Macmillan Publishers Ltd., copyright 2006 (*31*).

The results presented in this paper imply that the intermediate state is weak and forms potentially transient interactions that produce a molten globule. This is based on the large distance from the intermediate to the transition state toward unfolding and the low force needed to unfold. The authors suggest that this intermediate is on-pathway and assert that the data are consistent with the intermediate state observed in ensemble measurements. As a model system, RNase H provides further incentive to investigate the folding pathway of more complex systems and potentially protein domains with strategically placed DNA handles. Further, a more accurate description of the folding landscape of proteins and transition states could be made, because single-molecule methods can probe rare and potentially off-pathway transient states. In fact, another recent single-molecule experiment studied by FRET was able to accurately describe the ensemble of unfolded-state molecules (*28*).

Ankyrin as a Nanospring. Ankyrin repeats found in the genomes of prokaryotes, eukaryotes, and viruses are thought to function mainly in protein–protein interactions and as protein adaptors (*29, 30*). Individual repeats are composed of 33 amino acids that form two antiparallel α-helices bridged by a short unstructured loop. Ankyrin-containing proteins usually possess 4–6 ankyrin repeats and sometimes as many as 29. Approximately 24 repeats of ankyrin are sufficient to form one full helical turn (*31*). Ankyrin repeats have gained a significant amount of interest recently because of their putative function as a molecular spring (*29, 32*). Also of interest is the proposed ability of ankyrin repeats to fold and unfold as individual units.

In two recent studies, AFM-based force spectroscopy was used to investigate the unfolding behavior of individual ankyrin repeats (*30, 31*). In the report by Lee *et al.* (*31*), polypeptide constructs containing either 12 or 24 repeats of ankyrin were used in the pulling experiments. These molecules were attached to an *N*-nitrilotriacetic acid functionalized glass surface. The AFM cantilever was attached to the molecules by nonspecific adsorption to the tip, and force extension curves were recorded at a constant pulling rate by elevating the cantilever. The force *versus* extension curve was linear over a large range (Figure 6, panel c), an indication that in fact ankyrin is a hookean or linear spring. This is a unique finding because all previous studies of mechanical pulling of biological molecules showed nonlinear force *versus* extension curves and suggests that the linear behavior may be specially optimized for the cellular function of ankyrin. Because of extensive protein–protein interactions between repeats, this nanospring can withstand forces up to 600 pN.

After the initial extension of the molecule, subsequent unfolding occurred that formed a sawtooth pattern of evenly spaced events (blue curve in Figure 6, panel d). The distance between the unfolding events in the sawtooth pattern was calculated to be 12.4 nm, which matches the expected length of an unfolded individual ankyrin repeat when fully extended. These data indicate that after the ankyrin polymer is stretched to a point that intermolecular protein–protein contacts are broken, the repeats are then unfolded individually. These repeats are then able to refold as the extension is reduced and are shown to produce forces, 32 ± 8 pN, which are the same within error as the force necessary to unfold individual repeats, 37 ± 9 pN (Figure 6, panel d). These values are validated by another study that found the unfolding force of individual repeats to be 50 ± 20 pN (*30*).

Single-Molecule β-Galactosidase Activity. The kinetic mechanisms and processes that have formed the basis of enzymology continue to be of great interest for many researchers. The Michaelis–Menton equation, derived nearly a century ago, relates enzyme velocity as a function of substrate concentration and has been validated many times on the ensemble level. The enzyme β-galactosidase from *E. coli* was used to devise an experiment to test the Michaelis–Menton equation on the single-molecule level (*33*). β-Galactosidase, which catalyzes the hydrolysis of lactose, is a well-charac-

terized protein that exists as a tetramer containing one catalytic site per monomer.

An analogue, resorufin-β-D-galactopyranoside, was used as the substrate, because a fluorescent product, resorufin, is generated upon hydrolysis. Catalytic activity of β-galactosidase can then be monitored by the emergence of a fluorescence signal or burst upon excitation at 560 nm. A flexible poly(ethylene glycol) molecule linked to β-galactosidase was attached to a streptavidin-coated polystyrene bead, which was used to immobilize the protein to a glass coverslip surface (Figure 7, panel a). A confocal-type setup was used as the detection system for the experiments (Figure 2, panel a). A 560-nm laser was focused through the objective to excite the emergent fluorescent products from β-galactosidase.

The primary signal was the fluorescence fluctuations clearly above the background due to the production and release of the fluorescent product by a single enzyme (Figure 7, panel b). The autocorrelation function of the fluorescence time trajectory was calculated for several different substrate concentrations (Figure 7, panel c). When the concentration of the substrate is low, the function appears monoexponential, but when the concentration of the substrate is increased, the data seem multiexponential. This can be explained by the presence of conformational dynamics leading to dynamic disorder, which refers to rate fluctuations on time scales similar to or slightly longer than the reaction cycle. These different conformations of the protein potentially possess different affinities for the substrate. At low concentrations, enzyme substrate binding is rate limiting, which produces the monoexponential distribution because of a pseudo-first-order rate constant. As the substrate concentration is increased, the enzyme substrate binding is no longer rate limiting, and it is the catalytic activity or conversion of the substrate to resorufin that becomes rate limiting. Interconversion of the enzyme substrate complex to different conformations produces the dynamic disorder and the apparent multiexponential decay of the waiting time. These experiments validate the single-molecule Michaelis–Menten equation, which was recast to include dynamic disorder.

A correlation histogram of adjacent catalytic events of β-galactosidase and a similar histogram of events with long separation between events were constructed (not shown). The two histograms when compared are not identical, as would be expected if the individual molecules of β-galactosidase did not have a memory effect. A difference histogram constructed by subtracting the two previous histograms shows that short waiting times are more likely to be followed by short waiting times and likewise for long waiting times. This indicates that at least for β-galactosidase, a memory effect exists for enzymatic activity. Stated another way, whichever conformational state the enzyme is in for one event, it is more likely to be in that state upon binding of a subsequent substrate. This observation is a unique feature of single-molecule measurements and is completely obscured at the ensemble level.

Perspectives. Many interesting and important discoveries have been made with the help of single-molecule methods over the last few years. What does the future hold? Where does single-molecule science go from here? The instrumentation will undoubtedly improve to increase the spatial, molecular, and temporal resolution and to enable the simultaneous detection and correlation of multiple observables so that new kinds of questions can be asked and answered. One of the main hindrances with single-molecule fluorescence methods is the low concentration needed for distinguishing individual molecules. This makes some systems impossible to investigate because the dissociation constant is above the usable concentration of the system for optical detection. To overcome this, techniques are in development to encapsulate the system of interest and thus effectively increase the concentration (*34*–*36*). The potential for this and other similar methods is tremendous and ushers in the possibility of developing reaction containers usable for many applications (*37*). Traditional FRET experiments have been between one donor and one acceptor. As detection systems improve, more applications for three-color and multicolor FRET experiments will be employed (*38*, *39*). Combining different techniques such as

KEYWORDS

Fluorescence spectroscopy: A type of spectroscopy that measures the fluorescent signal or photons emitted by a fluorophore. Fluorescence spectroscopy has many uses for both ensemble and single-molecule applications.

Optical tweezers: A technique in which a bead or microsphere is trapped in a laser beam. Molecules can be attached to the trapped bead, which is then immobilized to another bead, a micropipet, or the surface. The beads can then be manipulated so that physical properties, such as force or molecular motions, can be measured.

Molecular motors: A broad classification of proteins that move along a scaffold such as DNA by using energy derived from ATP. Examples of molecular motors include helicases and proteins in the myosin family.

Single-molecule methods: These techniques are most useful for systems that cannot be synchronized in ensemble experiments, the investigation of heterogeneous systems, and the detection of rare events.

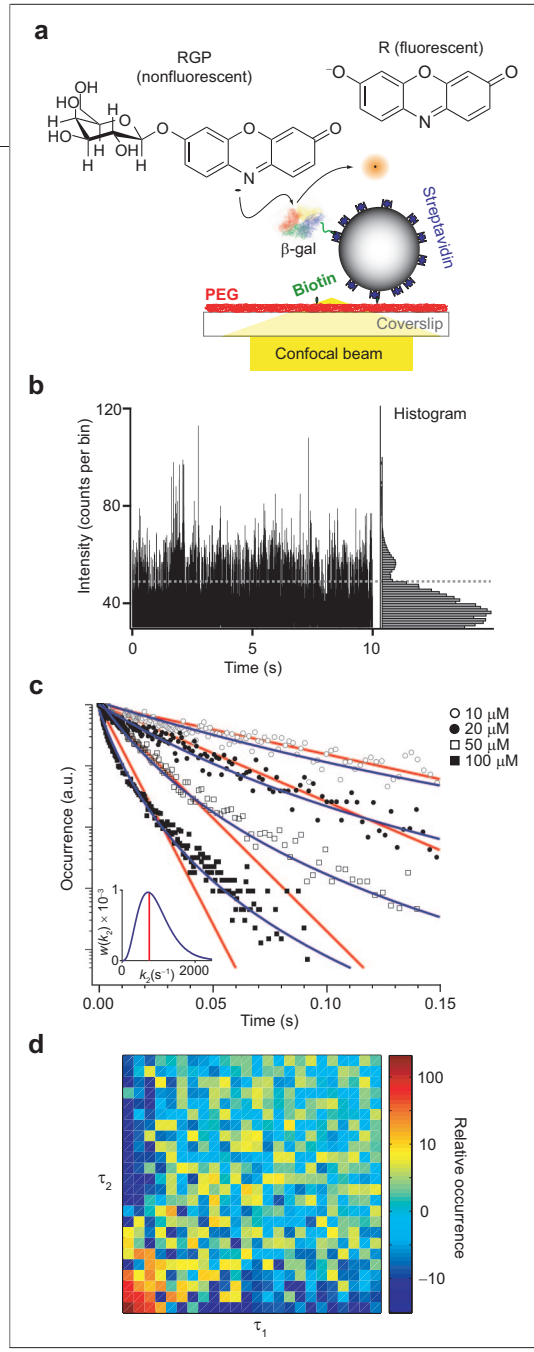

Figure 7. β-Galactosidase activity at the single-molecule level. a) Setup of the single-molecule experiments as described in the text. RGP = resorufin-β-D-galactopyranoside, R = resorufin. b) Representative intensity plot for an individual enzyme. The histogram indicates two regions: one is the noise, and the other is the fluorescent events of interest. c) Histogram plot of waiting times between adjacent events at different concentrations. The red line is a fit ignoring dynamic disorder, and the blue line is a fit that incorporates dynamic disorder. d) Difference histogram indicating memory effects of the enzyme. Short events are usually followed by short events and long events are usually followed by long events. Panels a–d reprinted by permission from Macmillan Publishers Ltd., copyright 2006 (*33*).

nanopore technology and optical traps (*40*) or fluorescence and force measurements will be extremely valuable (*41, 42*). The ultimate goal of single-molecule methods is to investigate biological processes *in vivo* by tracking the movement of individual molecules in two or three spatial dimensions (*43*). It will be exciting to see what the next few years produce.

REFERENCES

1. Allemand, J. F., Bensimon, D., and Croquette, V. (2003) Stretching DNA and RNA to probe their interactions with proteins, *Curr. Opin. Struct. Biol. 13*, 266–274.
2. Haustein, E., and Schwille, P. (2004) Single-molecule spectroscopic methods, *Curr. Opin. Struct. Biol. 14*, 531–540.
3. Michalet, X., Weiss, S., and Jager, M. (2006) Single-molecule fluorescence studies of protein folding and conformational dynamics, *Chem. Rev. 106*, 1785–1813.
4. Santos, N. C., and Castanho, M. A. (2004) An overview of the biophysical applications of atomic force microscopy, *Biophys. Chem. 107*, 133–149.
5. Bockelmann, U. (2004) Single-molecule manipulation of nucleic acids, *Curr. Opin. Struct. Biol. 14*, 368–373.
6. Bustamante, C., Chemla, Y. R., Forde, N. R., and Izhaky, D. (2004) Mechanical processes in biochemistry, *Annu. Rev. Biochem. 73*, 705–748.
7. Ha, T. (2004) Structural dynamics and processing of nucleic acids revealed by single-molecule spectroscopy, *Biochemistry 43*, 4055–4063.
8. Zhuang, X. (2005) Single-molecule RNA science, *Annu. Rev. Biophys. Biomol. Struct. 34*, 399–414.
9. Sako, Y., and Yanagida, T. (2003) Single-molecule visualization in cell biology, *Nat. Rev. Mol. Cell. Biol. Suppl.* SS1–SS5.
10. Lang, M. J., Asbury, C. L., Shaevitz, J. W., and Block, S. M. (2002) An automated two-dimensional optical force clamp for single molecule studies, *Biophys. J. 83*, 491–501.
11. Abbondanzieri, E. A., Greenleaf, W. J., Shaevitz, J. W., Landick, R., and Block, S. M. (2005) Direct observation of base-pair stepping by RNA polymerase, *Nature 438*, 460–465.
12. Moffitt, J. R., Chemla, Y. R., Izhaky, D., and Bustamante, C. (2006) Differential detection of dual traps improves the spatial resolution of optical tweezers, *Proc. Natl. Acad. Sci. U.S.A. 103*, 9006–9011.
13. Samori, B., Zuccheri, G., and Baschieri, R. (2005) Protein unfolding and refolding under force: methodologies for nanomechanics, *ChemPhysChem 6*, 29–34.
14. Ishihama, A. (2000) Functional modulation of *Escherichia coli* RNA polymerase, *Annu. Rev. Microbiol. 54*, 499–518.
15. Bai, L., Santangelo, T. J., and Wang, M. D. (2006) Single-molecule analysis of RNA polymerase transcription, *Annu. Rev. Biophys. Biomol. Struct. 35*, 343–360.
16. Kapanidis, A. N., Margeat, E., Laurence, T. A., Doose, S., Ho, S. O., Mukhopadhyay, J., Kortkhonjia, E., Mekler, V., Ebright, R. H., and Weiss, S. (2005) Retention of transcription initiation factor sigma70 in transcription elongation: single-molecule analysis, *Mol. Cell 20*, 347–356.
17. Herbert, K. M., La Porta, A., Wong, B. J., Mooney, R. A., Neuman, K. C., Landick, R., and Block, S. M. (2006) Sequence-resolved detection of pausing by single RNA polymerase molecules, *Cell 125*, 1083–1094.
18. Shaevitz, J. W., Abbondanzieri, E. A., Landick, R., and Block, S. M. (2003) Backtracking by single RNA polymerase molecules observed at near-base-pair resolution, *Nature 426*, 684–687.

19. Adelman, K., La Porta, A., Santangelo, T. J., Lis, J. T., Roberts, J. W., and Wang, M. D. (2002) Single molecule analysis of RNA polymerase elongation reveals uniform kinetic behavior, *Proc. Natl. Acad. Sci. U.S.A. 99*, 13538–13543.
20. Neuman, K. C., Abbondanzieri, E. A., Landick, R., Gelles, J., and Block, S. M. (2003) Ubiquitous transcriptional pausing is independent of RNA polymerase backtracking, *Cell 115*, 437–447.
21. Park, H., Ramamurthy, B., Travaglia, M., Safer, D., Chen, L. Q., Franzini-Armstrong, C., Selvin, P. R., and Sweeney, H. L. (2006) Full-length myosin VI dimerizes and moves processively along actin filaments upon monomer clustering, *Mol. Cell 21*, 331–336.
22. Yildiz, A., Forkey, J. N., McKinney, S. A., Ha, T., Goldman, Y. E., and Selvin, P. R. (2003) Myosin V walks hand-over-hand: single fluorophore imaging with 1.5-nm localization, *Science 300*, 2061–2065.
23. Yildiz, A., Park, H., Safer, D., Yang, Z., Chen, L. Q., Selvin, P. R., and Sweeney, H. L. (2004) Myosin VI steps via a hand-over-hand mechanism with its lever arm undergoing fluctuations when attached to actin, *J. Biol. Chem. 279*, 37223–37226.
24. Okten, Z., Churchman, L. S., Rock, R. S., and Spudich, J. A. (2004) Myosin VI walks hand-over-hand along actin, *Nat. Struct. Mol. Biol. 11*, 884–887.
25. Goedken, E. R., and Marqusee, S. (2001) Native-state energetics of a thermostabilized variant of ribonuclease HI, *J. Mol. Biol. 314*, 863–871.
26. Cecconi, C., Shank, E. A., Bustamante, C., and Marqusee, S. (2005) Direct observation of the three-state folding of a single protein molecule, *Science 309*, 2057–2060.
27. Tan, E., Wilson, T. J., Nahas, M. K., Clegg, R. M., Lilley, D. M., and Ha, T. (2003) A four-way junction accelerates hairpin ribozyme folding via a discrete intermediate, *Proc. Natl. Acad. Sci. U.S.A. 100*, 9308–9313.
28. Kuzmenkina, E. V., Heyes, C. D., and Nienhaus, G. U. (2006) Single-molecule FRET study of denaturant induced unfolding of RNase H, *J. Mol. Biol. 357*, 313–324.
29. Michaely, P., Tomchick, D. R., Machius, M., and Anderson, R. G. (2002) Crystal structure of a 12 ANK repeat stack from human ankyrinR, *EMBO J. 21*, 6387–6396.
30. Li, L., Wetzel, S., Pluckthun, A., and Fernandez, J. M. (2006) Stepwise unfolding of ankyrin repeats in a single protein revealed by atomic force microscopy, *Biophys. J. 90*, L30–L32.
31. Lee, G., Abdi, K., Jiang, Y., Michaely, P., Bennett, V., and Marszalek, P. E. (2006) Nanospring behaviour of ankyrin repeats, *Nature 440*, 246–249.
32. Howard, J., and Bechstedt, S. (2004) Hypothesis: a helix of ankyrin repeats of the NOMPC-TRP ion channel is the gating spring of mechanoreceptors, *Curr. Biol. 14*, R224–R226.
33. English, B. P., Min, W., van Oijen, A. M., Lee, K. T., Luo, G., Sun, H., Cherayil, B. J., Kou, S. C., and Xie, X. S. (2006) Ever-fluctuating single enzyme molecules: Michaelis-Menten equation revisited, *Nat. Chem. Biol. 2*, 87–94.
34. Boukobza, E., Sonnenfeld, A., and Haran, H. (2001) Immobilization in surface-tethered lipid vesicles as a new tool for single biomolecule spectroscopy, *J. Phys. Chem. B 105*, 12165–12170.
35. Lee, J. Y., Okumus, B., Kim, D. S., and Ha, T. (2005) Extreme conformational diversity in human telomeric DNA, *Proc. Natl. Acad. Sci. U.S.A. 102*, 18938–18943.
36. Okumus, B., Wilson, T. J., Lilley, D. M., and Ha, T. (2004) Vesicle encapsulation studies reveal that single molecule ribozyme heterogeneities are intrinsic, *Biophys. J. 87*, 2798–2806.
37. Noireaux, V., and Libchaber, A. (2004) A vesicle bioreactor as a step toward an artificial cell assembly, *Proc. Natl. Acad. Sci. U.S.A. 101*, 17669–17674.
38. Hohng, S., Joo, C., and Ha, T. (2004) Single-molecule three-color FRET, *Biophys. J. 87*, 1328–1337.
39. Clamme, J. P., and Deniz, A. A. (2005) Three-color single-molecule fluorescence resonance energy transfer, *ChemPhysChem 6*, 74–77.
40. Keyser, U. F., Koeleman, B. N., van Dorp, S., Krapf, D., Smeets, R. M. M., Lemay, S. G., Dekker, N. H., and Dekker, C. (2006) Direct force measurements on DNA in a solid-state nanopore, *Nat. Phys. 2*, 473–477.
41. Lang, M. J., Fordyce, P. M., Engh, A. M., Neuman, K. C., and Block, S. M. (2004) Simultaneous, coincident optical trapping and single-molecule fluorescence, *Nat. Methods 1*, 133–139.
42. Shroff, H., Reinhard, B. M., Siu, M., Agarwal, H., Spakowitz, A., and Liphardt, J. (2005) Biocompatible force sensor with optical readout and dimensions of 6 nm^3, *Nano Lett. 5*, 1509–1514.
43. Xie, X. S., Yu, J., and Yang, W. Y. (2006) Living cells as test tubes, *Science 312*, 228–230.